

Numerical simulations on the thermal management of Lithium-ion Battery pack based on liquid cooling

Nguyen Thanh Thuy¹, Nguyen ThiThuy Hang^{2*}

^{1,2}Faculty of automotive and power machinery engineering, Thai Nguyen University of Technology, Thai Nguyen, Vietnam

ABSTRACT:

Nowadays, Lithium-ion batteries are considered one of the main power supplies for electric vehicles due to their high energy density and long lifespan. However, lithium-ion batteries will be accompanied by a lot of heat during the charging and discharging process. Therefore, in order to make the battery power system available to play a better performance while ensuring security, it is necessary to optimize the design of the battery cooling solution. In this work, the computational fluid dynamics (CFD) method is used to investigate the thermal characteristic of the 18650 battery pack, which consists of 8 pieces of cells. The water-cooling performance of the battery pack is explored. Different water cooling strategies are investigated by changing the relative positions of the water flow inlet to acquire the best cooling way. The temperature distributions of the battery pack are discussed using transient simulation, and the results indicate that under the same inlet velocity, the maximum temperature at discharge rate = 2C is 300.223^oK for battery pack A and 300.332^oK for battery pack B. The cooling performance of the one-inlet is better than the case of the two-inlet.

KEYWORDS: Lithium-ion battery module; water immersion cooling, direct liquid cooling; ANSYS Fluent.

Date of Submission: 02-06-2023

Date of acceptance: 12-06-2023

I. INTRODUCTION

Given the growing concern over greenhouse gas emissions and the depletion of natural resources, there is a rising interest in the development and application of environmentally friendly energy solutions to address our energy challenges. Within the transportation industry, there is a shift away from conventional internal combustion engine vehicles, which currently consume 49% [2] of the world's fossil fuel oil resources and represent the largest energy-consuming sector experiencing rapid growth. Instead, eco-friendly energy vehicles are being embraced [3]. Many countries are now actively investing in achieving zero carbon emissions by 2050, with a particular focus on the electric car and battery industry, which plays a significant role in international agreements within the automotive sector [4].

In the last few years, Li-ion batteries have been considered the most suitable energy storage system in electric vehicles (EVs) due to several advantages such as high energy and power density, long cycle life, and low self-discharge compared to the other rechargeable battery types. In the general case, there is small space available for a power battery while designing the car. In addition, lithium-ion batteries will be accompanied by a lot of heat during the charging and discharging process. It is easy to lead to the accumulation of heat inside the battery and then affect battery performance and safety if the heat is not dissipated timely. If the heat dissipates unevenly, it will cause a large temperature difference inside the battery pack. The unevenness of the battery pack temperature field will cause unbalance of the battery modules and each cell's performance, and finally, affect the performance of the entire battery pack and security. Therefore, in order to make the battery power system available to play a better performance while ensuring security, it is necessary to optimize the design of the battery cooling solution. Therefore, battery thermal management systems (BTMSs) are required to dissipate the heat from the battery in time [5]. In the last decades, several types of BTMSs have been developed. Depending on the type of cooling medium, BTMSs can be categorized into four primary categories: an air cooling system (ACS) [6], a liquid cooling system [7], a phase-change-material (PCM) cooling system [8], and a heat pipe cooling system [9].

In this study, the computational fluid dynamics (CFD) method is used to investigate the thermal characteristic of the 18650 battery pack, which consists of 8 pieces of cells. The water-cooling performance of the battery pack is explored. Different water cooling strategies are investigated by changing the relative positions of the air flow inlet to acquire the best cooling way. The temperature distributions of the battery pack are discussed using transient simulation, and the results indicate that under the same inlet velocity, the

maximum temperature at discharge rate = 2C is 300.2230K for battery pack A and 300.3320K for battery pack B. The cooling performance of the one-inlet is better than the case of the two-inlet.

II. COMPUTATIONAL DOMAIN AND GOVERNING EQUATIONS

In the present study, the battery pack consists of several rows of 18650 batteries. Each row contains four batteries (as shown in Figure 1a). However, the computational domain is created, as shown in Figure 1b. The battery thermos-physical parameters are shown in Table 1 [12]. Along the flow direction, the cooling air just entering the battery pack conducts cooling air convection heat transfer on the battery surface, cooling the front module and heating the air itself; its cooling ability decreases, thus the temperature of the rear module will be higher than the front.

A calculation model is created, as shown in Figure 1. The battery pack consists of four rows of 18650 batteries. Each row contains two batteries. The battery thermos-physical parameters are shown in Table 1 [10]. Along the liquid flow direction, the cooling liquid just entering the battery pack conducts cooling liquid convection heat transfer on the battery surface, cooling the front module and heating the liquid itself; its cooling ability decreases, thus the temperature of the rear module will be higher than the front.

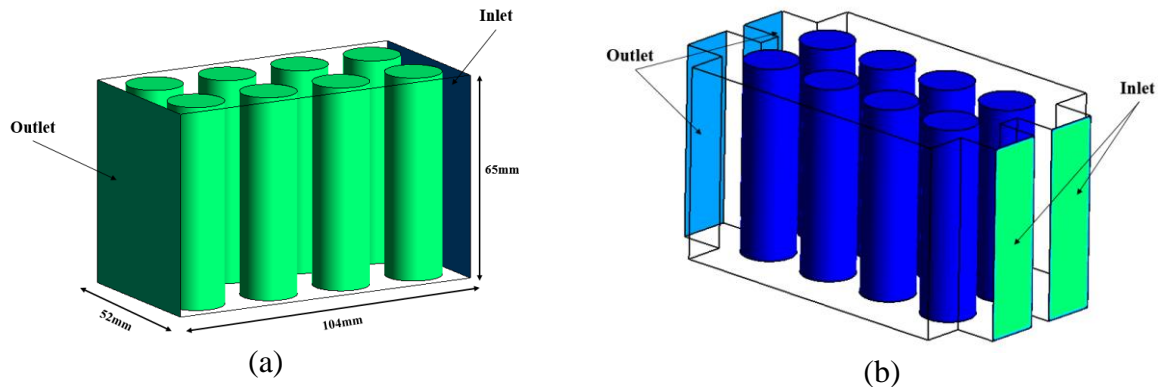


Figure 1. 3D computational model of: a) battery pack A; b) battery pack B

Table 1. Physical and thermal properties of the 18650 li-ion battery.

Rated Voltage (V)	3.6	Specific Heat Capacity ($J.kg^{-1}K^{-1}$)	1200	Density ($kg.m^{-3}$)	2722
Length	65	Diameter (mm)	18	Anisotropic thermal conductivity ($W.m^{-1}K^{-1}$)	$k_r = 0.2$ $k_z = 37.6$

The computational domain is discretized using structured hexahedral mesh elements (Figures 2a and 2b). The grid is clustered near the wall vicinity of batteries in order to take into account the strong gradients in this region. The middle plane of the battery module, where it was used to take place results, is shown in Figures 2c and 2d.

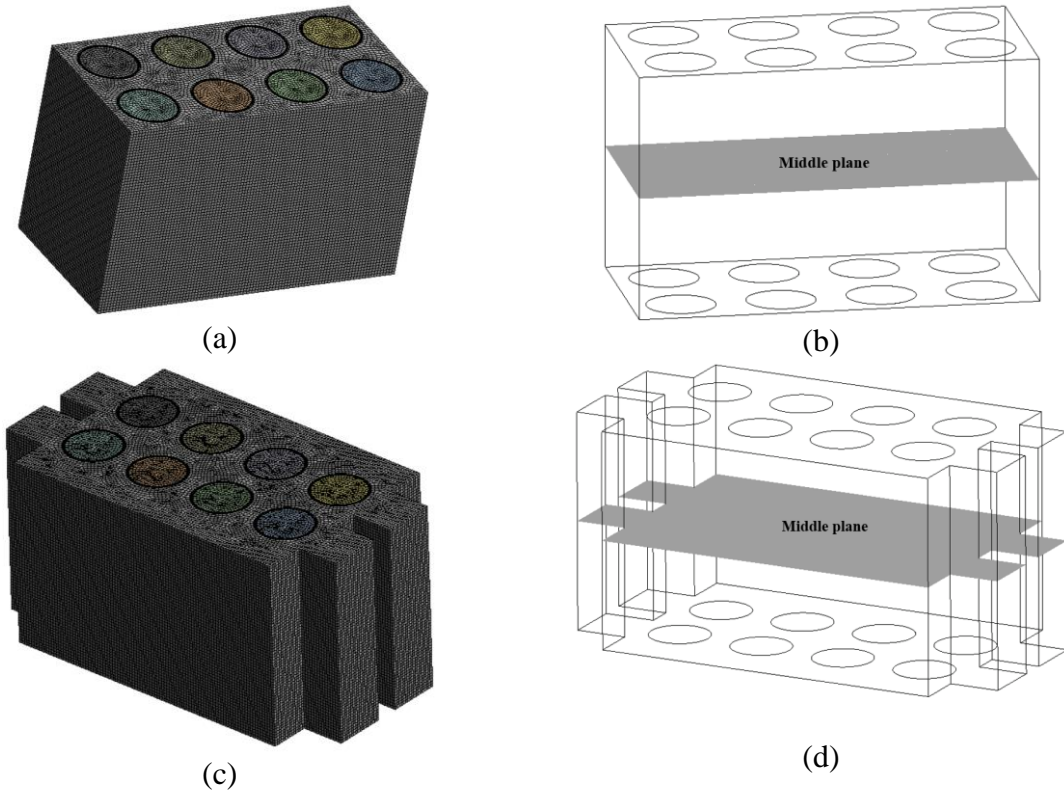


Figure 2. a) Close-up of mesh elements of battery pack A; b) The middle plane of battery pack A; c) Close-up of mesh elements of battery pack B; d) The middle plane of battery pack A

Then each cell on the middle plane of the battery pack A and B (see Figure 2) is numbered, as shown in Figure 3.

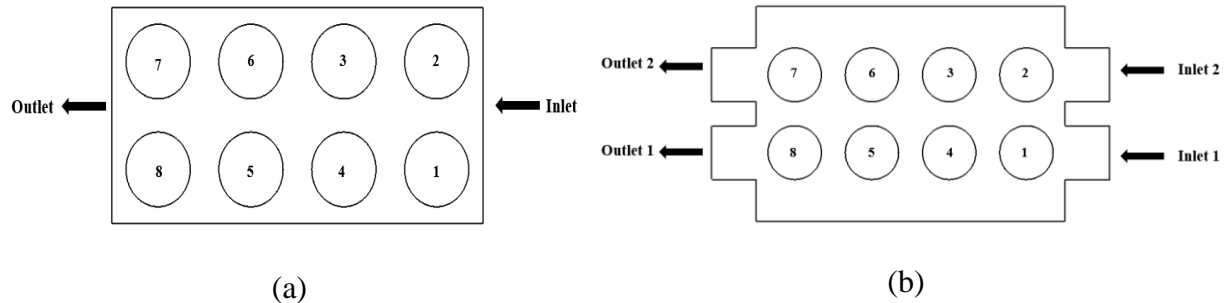


Figure 3. Schematic diagram of battery ID: a) battery pack A and b) battery pack B

In ANSYS-Fluent, the governing equations include the continuity, momentum, and energy equations. For the cooling air, these equations are shown as:

Continuity equation:

$$\frac{\partial \rho}{\partial t} + \nabla(\rho u) = 0 \quad (1)$$

Momentum equation:

$$\rho \frac{\partial u}{\partial t} + \rho u \cdot \nabla u = -\nabla p + \eta \nabla^2 u \quad (2)$$

Energy equation:

$$\frac{\partial(\rho c_p T)}{\partial t} + \nabla(\rho c_p u T) = \nabla(k \nabla T) \quad (3)$$

For the battery cell, the energy governing equation is expressed by:

$$\rho c_p \frac{\partial T}{\partial t} = \nabla(k \nabla T) + q \quad (4)$$

where ρ , c_p , T , p , k and q denote the density, specific heat, temperature, pressure, heat conductivity coefficient, the heat generation rate per unit volume of the battery, respectively.

A battery is considered as uniform a heat source. The heat generation rate per unit volume is expressed as equation 5.

$$q = a_0 + a_1t + a_2t^2 + \dots + a_nt^n \quad (5)$$

Where $a_0 \sim a_n$ are coefficients corresponding to the polynomial fitting method, q (W/m^3) is the heat generation rate and t (sec) is the time passed. These values were taken from [13]. The heat generation model is defined as an energy source term incorporated into CFD simulation using a user-defined function (UDF).

The standard k- ϵ model is selected which has been widely validated in modeling general low-speed and low-pressure flow around obstacles [12]. The k- ϵ turbulence model includes two equations for the turbulent kinetic energy k and the turbulent kinetic energy dissipation rate ϵ .

Turbulent kinetic energy equation:

$$\frac{\partial}{\partial t}(\rho k) + \frac{\partial}{\partial x_j}(\rho k u_j) = \frac{\partial}{\partial x_j} \left(\left(\mu + \frac{\mu_t}{\alpha_k} \right) \frac{\partial k}{\partial x_j} \right) + Gk + Gb - \rho \epsilon - YM + Sk \quad (6)$$

Turbulent kinetic energy dissipation equation:

$$\frac{\partial}{\partial t}(\rho \epsilon) + \frac{\partial}{\partial x_j}(\rho \epsilon u_j) = \frac{\partial}{\partial x_j} \left(\left(\mu + \frac{\mu_t}{\alpha_\epsilon} \right) \frac{\partial \epsilon}{\partial x_j} \right) + C1\epsilon \frac{\epsilon}{k} (Gk + C3\epsilon Gb) - \rho C2\epsilon \frac{\epsilon^2}{k} + S\epsilon \quad (7)$$

where k and ϵ denote turbulent kinetic energy and turbulent dissipation rate, respectively.

The settings for the boundary conditions are as the following. The inlet and outlet are set as the velocity inlet and the pressure outlet, respectively. The top, bottom and both sides are defined as walls. In addition, the interfaces between batteries and fluid are defined as coupled walls.

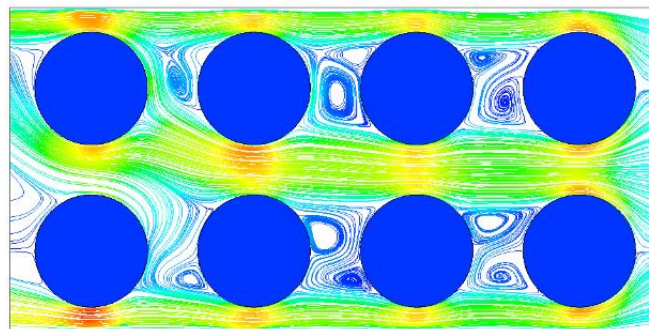
The convergence criterion, i.e., the scaled residual, for both mass, momentum and energy equations are set to 10⁻⁵ and 10⁻⁶, respectively, in each time step of the flow.

To analyze mesh independency, three mesh sizes are tested for both computational domains. The mesh density was almost doubled in each refinement. Finally, the mesh size for battery packs A and B are, respectively 507000 elements and 698880 elements.

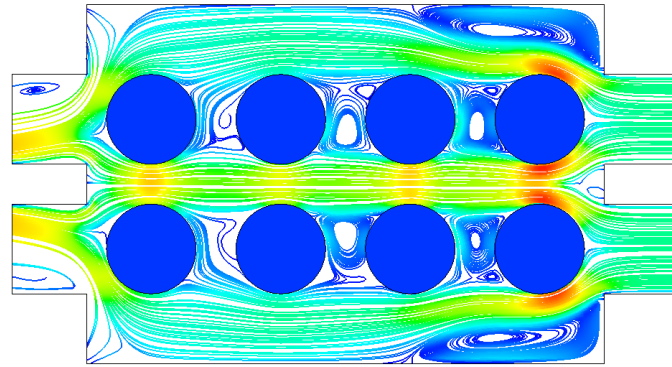
The effects of time steps on the results are also tested using 50, 150 and 200 steps per cycle. Finally, 150 steps per cycle are used for the simulation in the transient regime.

IV. RESULTS AND DISCUSSION

Figure 4 shows the streamlines of the battery module. Figure 4. (a) shows that the flow resistance and the turbulence degree are bigger, and the heat transfer capacity of the battery and cooling liquid flow increase, which improves the cooling performance of the pack. Figure 4 (b) shows that the flow is smooth, and the fluid resistance and the degree of turbulence are small in the two-inlet design. As a result, we can see in Figure 5 and conclude that the cooling performance of one-inlet (see Fig 4 (a)) is obviously better than the case of two-inlet (in Figure 4(b)), and the temperature difference between the front row and the rear row is little. Battery consistency is good. However, it can be seen in both designs (one-inlet and two-inlet) that the whole battery pack is surrounded by the cooling liquid evenly and has a good heat exchange capability.



(a)



(b)
Figure 4. Streamlines of (a) battery pack A and (b) battery pack B

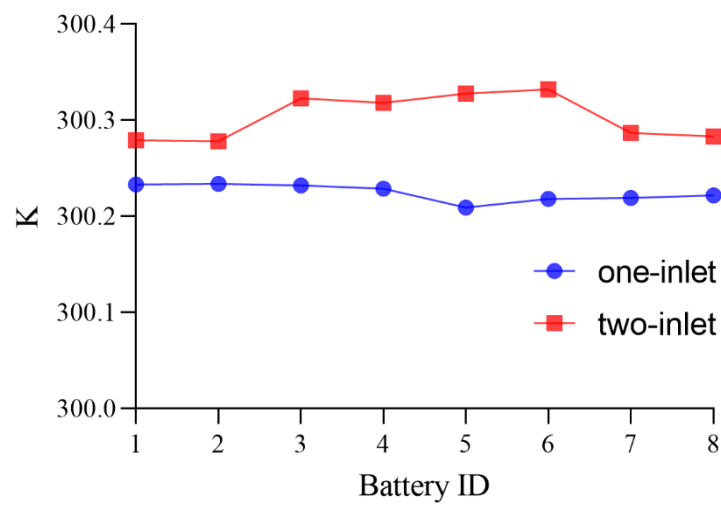
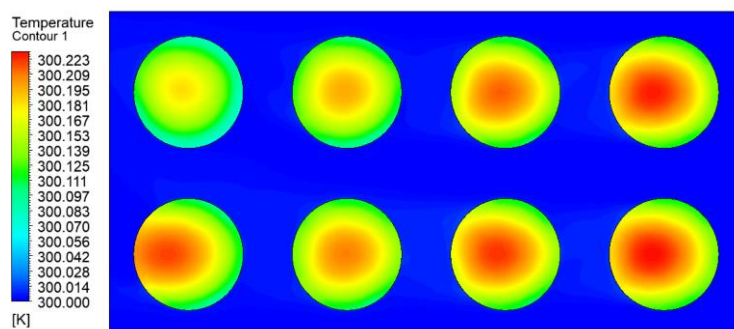


Figure 5. Relationship between temperature and inlet quantity for the same inlet velocity

Figure 6 shows the evolution and distribution of temperature in the battery pack of battery pack A and battery pack B. Comparing the one-inlet design with double - inlet design in figure.6(a) and (b), we can find that the battery far from the inlet, cooling performance of the one-inlet design is superior to the two-inlet design; while for battery near the inlet, two-inlet design is better; In addition, one-inlet design is beneficial to battery consistency.



(a)

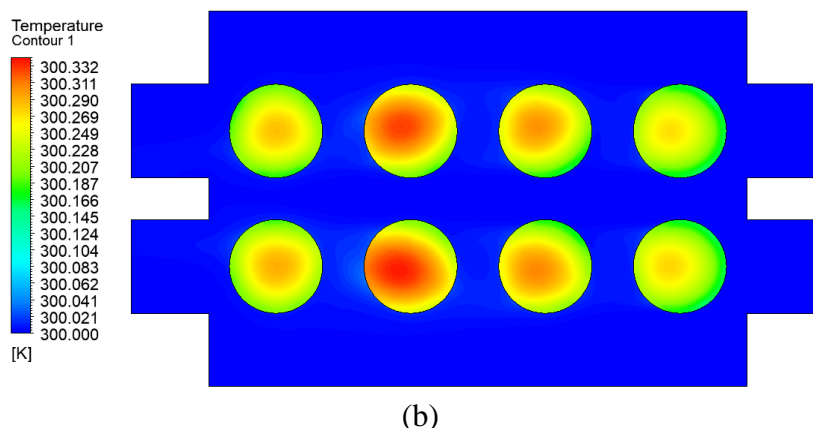


Figure 6. The evolution and distribution of temperature in battery pack of: battery pack A and (b) battery pack B

V. CONCLUSION

WIn this paper, a numerical study was conducted to determine the efficiency of water cooling of Lithium-ion batteries at different inlet designs (one inlet and two inlets). The main conclusions of this work can be summarized as follows.

- Under the same inlet velocity, the maximum temperature at discharge rate = 2C is 300.2230K for battery pack A and 300.3320K for battery pack B.

- The cooling performance of one-inlet (battery pack A) is obviously better than the case of two-inlet (battery pack B), and battery pack A exhibits a smaller thermal gradient between the front and rear battery rows.

In the future, the primary focus of water immersion cooling system design will be to enhance the temperature uniformity within battery packs. One effective approach to achieve this is by incorporating multiple inlet and outlet points along with cross-flow design. By implementing a novel inlet/outlet structure, a more consistent and stable flow of water can be ensured within the battery pack. Another potential solution for immersion cooling is the utilization of phase change emulsion. This innovative approach takes advantage of the higher specific heat capacity and the phase change process of the emulsion, effectively reducing the temperature difference within the battery pack.

Acknowledgment

The authors would like to express our gratitude to the Thai Nguyen University of Technology for support of this work.

REFERENCES

- [1]. Chen, Y., Kang, Y., Zhao, Y., Wang, L., Liu, J., Li, Y., Liang, Z., He, X., Li, X., Tavajohi, N., and Li, B., 2021, "A Review of Lithium-Ion Battery Safety Concerns: The Issues, Strategies, and Testing Standards," *Journal of Energy Chemistry*, 59, pp. 83–99.
- [2]. United States Environmental Protection Agency, 2021, "Sources of Greenhouse Gas Emissions" [Online]. Available: <https://www.epa.gov/ghgemissions/sources-greenhouse-gas-emissions>. [Accessed: 26-Feb-2021].
- [3]. Amjad, S., Neelakrishnan, S., and Rudramoorthy, R., 2010, "Review of Design Considerations and Technological Challenges for Successful Development and Deployment of Plug-in Hybrid Electric Vehicles," *Renewable and Sustainable Energy Reviews*, 14(3), pp. 1104–1110.
- [4]. Roe, C., Feng, X., White, G., Li, R., Wang, H., Rui, X., Li, C., Zhang, F., Null, V., Parkes, M., Patel, Y., Wang, Y., Wang, H., Ouyang, M., Offer, G., and Wu, B., 2022, "Immersion Cooling for Lithium-Ion Batteries – A Review," *Journal of Power Sources*, 525, p. 231094.
- [5]. Lu, L., Han, X., Li, J., Hua, J., and Ouyang, M., 2013, "A Review on the Key Issues for Lithium-Ion Battery Management in Electric Vehicles," *Journal of Power Sources*, 226, pp. 272–288.
- [6]. Fan, L., Khodadadi, J. M., and Pesaran, A. A., 2013, "A Parametric Study on Thermal Management of an Air-Cooled Lithium-Ion Battery Module for Plug-in Hybrid Electric Vehicles," *Journal of Power Sources*, 238, pp. 301–312.
- [7]. Panchal, S., Khasow, R., Dincer, I., Agelin-Chaab, M., Fraser, R., and Fowler, M., 2017, "Thermal Design and Simulation of Mini-Channel Cold Plate for Water Cooled Large Sized Prismatic Lithium-Ion Battery," *Applied Thermal Engineering*, 122, pp. 80–90.
- [8]. Rao, Z., and Wang, S., 2011, "A Review of Power Battery Thermal Energy Management," *Renewable and Sustainable Energy Reviews*, 15(9), pp. 4554–4571.
- [9]. Putra, N., Ariantara, B., and Pamungkas, R. A., 2016, "Experimental Investigation on Performance of Lithium-Ion Battery Thermal Management System Using Flat Plate Loop Heat Pipe for Electric Vehicle Application," *Applied Thermal Engineering*, 99, pp. 784–789.
- [10]. Behi, H., Karimi, D., Behi, M., Ghanbarpour, M., Jaguemont, J., Sokkeh, M. A., Gandoman, F. H., Berecibar, M., and Mierlo, J. V., 2020, "A New Concept of Thermal Management System in Li-Ion Battery Using Air Cooling and Heat Pipe for Electric Vehicles," *Applied Thermal Engineering*, 174, p. 115280.
- [11]. Hwang, F. S., Confrey, T., Scully, S., Callaghan, D., Nolan, C., Kent, N., and Flannery, B., 2020, "MODELLING OF HEAT GENERATION IN AN 18650 LITHIUM-ION BATTERY CELL UNDER VARYING DISCHARGE RATES," *Proceeding of 5th Thermal and Fluids Engineering Conference (TFEC)*, Begellhouse, New Orleans, LA, USA, pp. 333–341.
- [12]. Xing, J., Liu, Z., Huang, P., Feng, C., Zhou, Y., Zhang, D., and Wang, F., 2013, "Experimental and Numerical Study of the Dispersion of Carbon Dioxide Plume," *Journal of Hazardous Materials*, 256–257, pp. 40–48.